Universiteit Utrecht

Opleiding Natuur- en Sterrenkunde

Correlations between flow harmonics in Pb-Pb collisions at $\sqrt{s_{NN}} = 2.76$ TeV

Bachelor Thesis

Marten Barel

Supervisors:

Prof. Dr. Raimond Snellings
Universiteit Utrecht

Jacopo Margutti, MSc
Universiteit Utrecht

June 14, 2017

Abstract

The Quark-Gluon Plasma (QGP) is the object of study of the ALICE experiment. To get a grip on some of its properties, the so-called *flow harmonics* are studied. In this thesis the values of some of these harmonics, and the correlations between them are estimated using data recorded with the ALICE detector from Pb-Pb collisions with energies of $\sqrt{s_{NN}} = 2.76$ TeV. An algorithm for the calculations needed to obtain these correlations, as presented in Ref.[1], is tested. An overview of the detector used to record the data, and of the mathematics used to estimate the flow harmonics and their correlations is given. The results show that the harmonics themselves behave as expected and that the algorithm did not produce accurate results. Some suggestions are given as to why it didn't and what could be done to improve the results.

Contents

1 Introduction

In the field of high energy physics many different topics are being researched. Some of these are the nature of sub-atomic particles or the nature of the early universe. One of the objects of study is the so-called quark-gluon plasma, which is theorized to have been the state in which our universe resided at times shorter than $t \sim 10^{-5}$ seconds and temperatures of at least $T \sim 2 \times 10^{12}$K [2]. In the lab the quark-gluon plasma is created by colliding heavy ions at very high energies, in the case of the LHC lead ions. How exactly this is done, will be explained in Section 2. Many models exist that describe the way the quark-gluon plasma, or QGP, behaves and do so quite successfully. The problem that remains is that the initial conditions of these models can still be varied and produce accurate predictions of how the QGP behaves. In order to further restrict these initial values we can calculate the correlations between the flow harmonics. What these are and why they are important will be explained in Section 3. The methods for calculating these correlations have already been developed to some extent. In particular I will be looking at an algorithm which is introduced in Ref.[1] and can be used in order to calculate these correlations. This then brings us to my research question:

Is this algorithm a good method for calculating correlations in flow harmonics?

What defines a good method? In this case the algorithm can be considered good if, first, it makes accurate calculations of what the correlations are. Second, if it is compact, so that it does not need many lines of code to implement. And finally if it is fast, it is of little use to have a fancy method for calculating the correlations if it takes really long to do so. With this we can define several secondary questions:

- Is this algorithm fast?
- Is this algorithm compact?
- Is this algorithm accurate?

Whether or not this algorithm satisfies these conditions will be explored in this thesis. I will start off with an explanation of the detector, focusing on the parts that were of most importance to my research. Then I will explore the mathematics behind the flow harmonics, starting off with integrated and differential flow, then moving on to the algorithm itself. After that I will show the results for the integrated and differential flow, and those of the algorithm itself. Finally I will draw conclusions and discuss the results in more detail, also giving some suggestions for improvement or future research.

2 Experiment

In order to calculate the correlations and test the algorithm data is needed. The data used in this thesis was recorded by the ALICE detector, located at CERN near Geneva, Switzerland. It is one of the experiments being conducted at the Large Hadron Collider, or LHC. The LHC is a circular accelerator with a circumference of 27 km, and as such is currently the largest and most powerful particle accelerator in the world. Currently the LHC has achieved collisions with energies up to 13 TeV in the center-of-mass system [3].

2.1 The ALICE detector

In this section I will give a brief overview of the detector that recorded the data used in this thesis, for a more detailed description see Ref.[4]. ALICE, a shorthand for A Large Ion Collider Experiment, is a heavy-ion detector built in order to study the particles produced during Pb-Pb collisions, which will originate from the expanding QGP created after the impact of two ions. As such it capable of handling high multiplicities, being optimized for $\mathrm{d}N/\mathrm{d}\eta = 4000$, but tested with simulations up to $\mathrm{d}N/\mathrm{d}\eta = 8000$. An overview of the layout of the detector is given in Fig.1. Starting from the impact point, the innermost part of the detector is the ITS, or inner tracking system. It consists of the Silicon Pixel Detector (SPD), the Silicon Drift Detector (SDD) and the Silicon Strip Detector (SSD), having two layers of each type starting with the SPD followed by the SDD and the SSD in that order. The main tasks of the ITS are: to localize the impact point with a resolution better than 100 μm, to aid in the reconstruction of secondary decays, and to track and identify particles with a momentum lower than 200 MeV/c. This is done to improve the momentum and angle resolution of particles reconstructed by the Time Projection Chamber (TPC) and to reconstruct particles traversing the dead regions of the TPC. It covers a pseudo-rapidity range of $|\eta| < 0.9$ for all vertices within the interaction diamond. This is region around the interaction point with a length of 5.3 cm in either beam directions and 1 cm transverse to the beam measured from the center of the interaction point, thus forming a diamond shape. Directly surrounding the ITS is the TPC, this is the main tracking detector and it is optimized to provide charged-particle momentum measurements. As such it has good two-track separation, particle identification, and vertex determination. It can fully cover the entire azimuthal plane, with the exception of some deadzones. It has a psuedo-rapidity range of $|\eta| < 0.9$ for full radial tracks (tracks with matches in the ITS, TRD and TOF detectors); it can also cover reduced tracks (tracks that are not fully radial) up to $|\eta| = 1.5$, and covers a large p_{T} range of about 0.1 GeV/c to 100 GeV/c with good momentum resolution. Further outward there are more detectors, the Transistion Radiation Detector (TRD), the Time-Of-Flight (TOF) detector, the High-Momentum Particle Identifcation Detector (HMPID), PHOton Spectrometer (PHOS) and ElectroMagnetic CALorimeter (EMCAL). These detectors are important to the research being conducted at ALICE, but are not of interest for this thesis, for more information on these detectors see Ref.[4].
In the beam directions, both forward and back, several more detectors are found. For this thesis the V0 detector is of the most interest, because it is used to estimate the centrality of the collisions. It is a small angle detector consisting of two parts, V0A and V0C on opposite ends of the interaction point. Each of these consists of arrays of scintillation counters. The

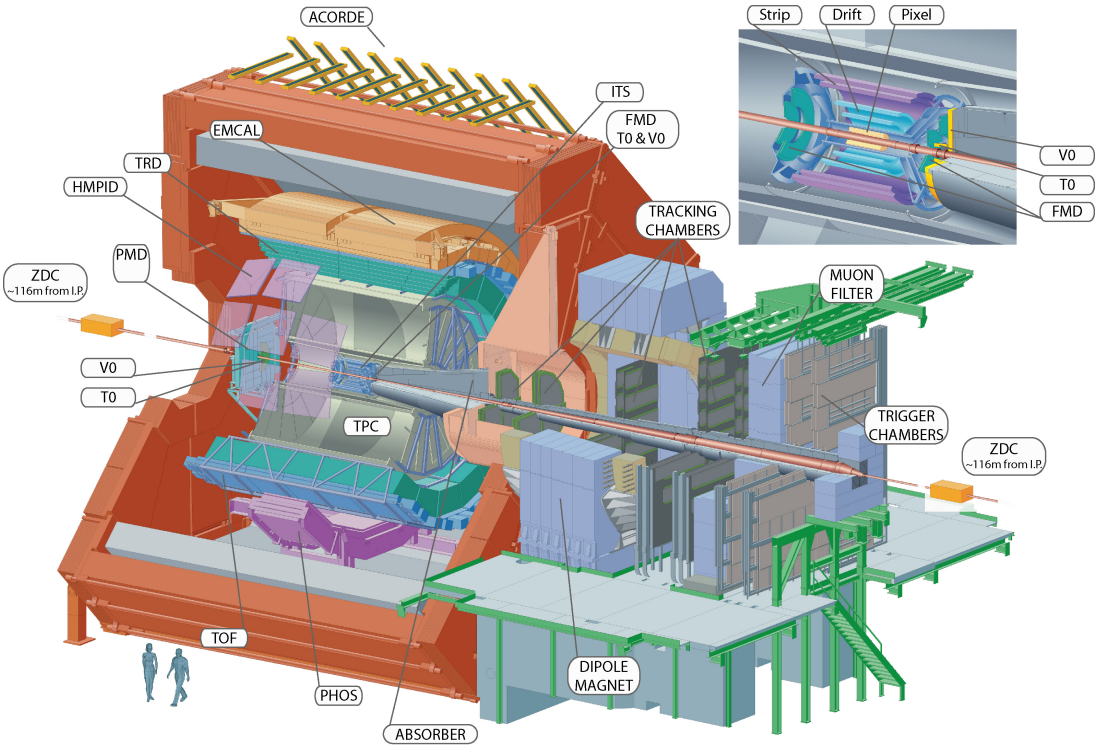

Figure 1: Overview of the ALICE detector layout, with in the top right a close up of the ITS. [5]

V0 serves several purposes, it provides triggers for the central barrel detectors, such as the ITS and the TPC, in pp and A-A collisions. The V0 also serves as an indicator of the centrality of the collision by recording the multiplicity of the event. Cuts can be made on the total number of fired counters and on the total charge in order to achieve centrality triggers. There are three different triggers using this method, the multiplicity, semi-central and central triggers.

2.2 Data and data selection

For this thesis data recorded from a run in 2010, with Pb-Pb collisions with energies of $\sqrt{s_{NN}} = 2.76$ TeV, is used. In this thesis only the tracks of charged particles were being analysed. The tracks that were used for analysis are those with hits in both the ITS and TPC detectors. In particular tracks that originated from the primary vertex, and without any kinks, having one or multiple kinks in the track would indicate a scattering or that a secondary decay has occurred. The total number of events is a little under 16 million. The centrality estimation was done using the V0 detector. Some further selection was made on the data in the form of centrality and pseudo-rapidity cuts. For the correlations calculations were made for centralities up to 70%. For higher centrality percentiles there is too much contamination from secondary collisions such as beam-gas collisions, which will lead to inaccurate results. A centrality cut already existed in the data around the 90% mark. Events with a centrality of 0% were also excluded, because many of these are events without any actual tracks, leading to errors in the program when it ran. A further cut was made on the data via the pseudo-

rapidity parameter, accepting only tracks with $-0.8 < \eta < 0.8$. This is mostly due to limited coverage of the TPC which covers $-0.9 < \eta < 0.9$ for full radial tracks as mentioned above. A cut was also made on the transverse momentum p_{T}, accepting only tracks with $0.2 < p_{\mathrm{T}} < 50$ GeV/c. For the calculation on the differential flow, as explained in Section 3, the same cuts as before on p_{T} and η were made. This time looking only at events with centralities between 20% and 30%.

2.3 Methods

Before we get into the theory from which the algorithm is derived, some explanation as to how the data was processed is in order. For all the calculations ROOT was used. ROOT is a modular scientific software framework. It provides all the functionalities needed to deal with big data processing, statistical analysis, visualisation and storage. It is mainly written in C++ but integrated with other languages such as Python and R, see also Ref.[6]. For this thesis C++ was used. For the calculations of the flow harmonics new code was written, for the calculation of the correlations between the harmonics using the algorithm, a code package provided by the authors of the algorithm was used, for more information on the algorithm, see Section 3.2.

3 Theory

In this section the mathematics for calculating the correlations will be covered. Starting off with an explanation of integrated and differential flow as described in Ref.[7], then moving on to the algorithm itself. In order to explain how I used this algorithm I will also be explaining the way these correlations can be calculated directly.

3.1 Integrated and differential flow

In this section I will introduce the methods for calculating integrated and differential flow as put forward in Ref.[7]. We begin with an explanation as to what flow is in the context of this thesis. Flow gives a description of the collective expansion of the QGP in the plane perpendicular to the beam; As such it is also known as transverse flow[8]. This transverse flow can be split into two parts, central flow and anisotropic flow, the part we are interested in is anisotropic flow. Anisotropic flow is a way to quantify the anisotropies in the azimuthal distribution of final-state particles. One way to interpret these anisotropies is as a response of the QGP to the anisotropies in the initial geometry, as such it is highly susceptible to the properties of the QGP at an early time of its evolution. It can be characterized by coefficients of a Fourier expansion of the azimuthal dependence of the invariant yield of particles relative to the reaction plane:

$$E\frac{d^3N}{d^3p} = \frac{1}{2\pi}\frac{d^2N}{p_{\mathrm{T}}dp_{\mathrm{T}}dy}[1 + \sum_{n=1}^{\infty} 2v_n \cos\left(n(\phi - \Psi_{\mathrm{RP}})\right)]. \tag{1}$$

Here E is the energy of the particle, p_{T} is the transverse momentum, ϕ is its azimuthal angle, y is the rapidity, and Ψ_{RP} is the reaction plane angle; see Fig.2. In Eq.1 we see the

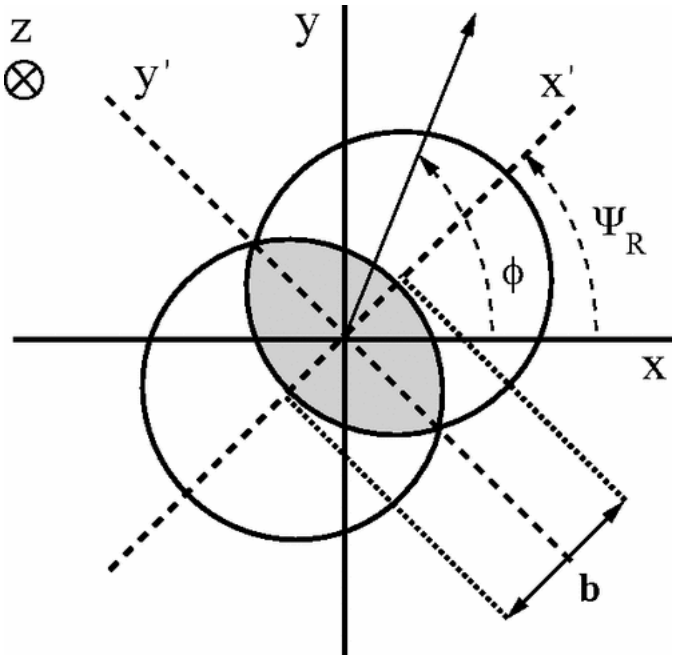

Figure 2: Schematic overview of a non-central collision in the transverse plane. [7]

coefficients labelled v_n, the first coefficient v_1 is often called directed flow, and v_2 is called elliptic flow. These coefficients are what we call the *flow harmonics*. We can look at either the p_{T} dependence of these coefficients, in which case we talk about *differential flow*, or at the centrality dependence, the so-called *integrated flow*. The values of these coefficients are estimated using multi-particle azimuthal correlations. In order to calculate these correlations without having to deal with non-flow contributions multi-particle cumulants are used. One of the major problems in using these cumulants is the large amount of computing power needed to go over all possible particle multiplets. So in order to avoid this problem we can express the cumulants in terms of moments of the magnitude of the corresponding flow vector Q_n, defined as:

$$Q_n \equiv \sum_{i=1}^{M} e^{in\phi_i}, \tag{2}$$

where M is the number of particles. Using the approach put forward in Ref.[7] the cumulants are calculated directly from the data without any approximations. As such they are called *direct cumulants* or *Q-cumulants*. In this thesis all calculations of flow or flow correlations were done using 2-particle and 4-particle correlations. They are obtained by first averaging over all particles in a given event and then averaging over all events. This latter uses weights depending on event multiplicity. Single-event average 2- and 4-particle correlations are defined as:

$$\langle 2 \rangle \equiv \langle e^{in(\phi_1-\phi_2)} \rangle \equiv \frac{1}{P_{M,2}} {\sum_{i,j}}' e^{in(\phi_i-\phi_j)}, \tag{3}$$

$$\langle 4 \rangle \equiv \langle e^{in(\phi_1+\phi_2-\phi_3-\phi_4)} \rangle \equiv \frac{1}{P_{M,4}} {\sum_{i,j,k,l}}' e^{in(\phi_i+\phi_j-\phi_k-\phi_l)}, \tag{4}$$

where $P_{n,m} = n!/(n-m)!$, and the prime in the sum, i.e. $\sum_{i,j,k,l}{}'$, means that $i \neq j \neq k \neq l$. The second step involves averaging over all events:

$$\langle\langle 2\rangle\rangle \equiv \langle\langle e^{in(\phi_1-\phi_2)}\rangle\rangle \equiv \frac{\sum_{events}(W_{(2)})_i\langle 2\rangle_i}{\sum_{events}(W_{(2)})_i}, \tag{5}$$

$$\langle\langle 4\rangle\rangle \equiv \langle\langle e^{in(\phi_1+\phi_2-\phi_3-\phi_4)}\rangle\rangle \equiv \frac{\sum_{events}(W_{(4)})_i\langle 4\rangle_i}{\sum_{events}(W_{(4)})_i}, \tag{6}$$

the double brackets indicate an average, first over all particles and then over all events. $W_{(2)}$ and $W_{(4)}$ are the event weights, which are used to minimize the effect of multiplicity variations in the event sample on the correlations. The weights are defined as:

$$W_{(2)} \equiv M(M-1), \tag{7}$$

$$W_{(4)} \equiv M(M-1)(M-2)(M-3). \tag{8}$$

This definition of the weights takes into account the number of different 2- and 4-particle combinations in an event with multiplicity M. Using the definitions above we can now define the 2- and 4-particle cumulants, the 2-particle cumulant is simply the event averaged 2-particle correlation defined in Eq.5:

$$c_n\{2\} = \langle\langle 2\rangle\rangle, \tag{9}$$

and the 4-particle cumulant is given by:

$$c_n\{4\} = \langle\langle 4\rangle\rangle - 2\cdot\langle\langle 2\rangle\rangle^2. \tag{10}$$

From here we can now calculate the actual flow harmonics v_n, we can use different order cumulants to estimate the value of the same harmonic, in particular:

$$v_n\{2\} = \sqrt{c_n\{2\}}, \tag{11}$$

$$v_n\{4\} = \sqrt[4]{-c_n\{4\}}, \tag{12}$$

where the number in braces behind the v_n is used to denote the order of cumulant used for estimation of the flow harmonic. Having defined all this we can now get into the theory of integrated and differential flow.

3.1.1 Integrated flow

We begin by showing how the integrated or reference flow is calculated, once again following Ref.[7]. We begin by separating the diagonal and off-diagonal terms in $|Q_n|^2$:

$$|Q_n|^2 = \sum_{i,j=1}^{M} e^{in(\phi_i-\phi_j)} = M + \sum_{i,j}{}' e^{in(\phi_i-\phi_j)}, \tag{13}$$

where the factor M in the last term appears for all instances that $i = j$, and the final sum once again has $i \neq j$. From this we now easily obtain $\langle 2 \rangle$:

$$\langle 2 \rangle = \frac{|Q_n|^2 - M}{M(M-1)}. \tag{14}$$

We can now use Eq.5, Eq.9, and Eq.11 to find the 2-particle harmonics $v_n\{2\}$. Something similar to this can be done in order to obtain the event averaged 4-particle correlation, we start with the decomposition of $|Q_n|^4$, for the full decomposition see Ref.[7]:

$$|Q_n|^4 = Q_n Q_n Q_n^* Q_n^* = \sum_{i,j,k,l=1}^{M} e^{in(\phi_i + \phi_j - \phi_k - \phi_l)}. \tag{15}$$

From its decomposition we can now obtain the single-event averaged 4-particle correlation:

$$\langle 4 \rangle = \frac{|Q_n|^4 + |Q_{2n}|^2 - 2 \cdot \mathfrak{Re}[Q_{2n} Q_n^* Q_n^*]}{M(M-1)(M-2)(M-3)} - 2\frac{2(M-2) \cdot |Q_n|^2 - M(M-3)}{M(M-1)(M-2)(M-3)}, \tag{16}$$

from here we can obtain $\langle\langle 4 \rangle\rangle$ by using Eq.6 and Eq.8. Using this and the 2-particle correlation from Eq.5 we can now obtain the 4-particle cumulant $c_n\{4\}$ as defined in Eq.10, and from it $v_n\{4\}$ using Eq.12.

3.1.2 Differential flow

Using the formulas from the previous section an estimation can be made of the integrated or reference flow. The reason it is called reference flow is because it is used as a reference when calculating the differential flow. In order to calculate the differential flow we need to label some particles of interest (POIs) and reference flow particles (RFPs). In this thesis the POIs were particles that fell within a given transverse momentum range. Starting with $p_{\mathrm{T}} = 0.2$ GeV/c and moving up in incremental steps to $p_{\mathrm{T}} = 50$ GeV/c, all calculations were done for events within the 20-30% centrality range. The RFPs were simply all particles within the same centrality range. Now we can estimate the differential flow of the POIs using the reference flow calculated using the RFPs. For this section I will only cover the 2-particle correlations, since these were the only ones I used for calculating the differential flow. We start of by defining the *reduced* 2-particle azimuthal correlation:

$$\langle 2' \rangle \equiv \langle e^{in(\psi_1 - \phi_2(} \rangle \equiv \frac{1}{m_p M - m_q} \sum_{i=1}^{m_p} {\sum_{j=1}^{M}}' e^{in(\psi_i - \phi_j)}, \tag{17}$$

where m_p is the total number of POIs, which can also include some particles labelled as RFPs. m_q is the total number of particles that are both a POI and a RFP, so for this thesis $m_p = m_q$, because all particles that are being looked at are RFPs. M is the total number of particles labelled as RFP, some of which are also POIs. ψ_i is the azimuthal angle of the i-th particle labelled as POI. ϕ_j is the azimuthal angle of the j-th particle labelled as RFP. The prime after the summation sign once again denotes a sum with all indices taken different.

The event averaged reduced 2-particle correlation is given by:

$$\langle\langle 2' \rangle\rangle \equiv \frac{\sum\limits_{events} (w_{(2')})_i \langle 2' \rangle_i}{\sum\limits_{events} (w_{(2')})_i}, \tag{18}$$

where the weights are defined as:

$$w_{(2')} \equiv m_p M - m_q. \tag{19}$$

From this we now get the differential 2-particle cumulant $d_n\{2\}$:

$$d_n\{2\} = \langle\langle 2' \rangle\rangle. \tag{20}$$

Now the 2-particle differential flow $v'_n\{2\}$ is given by:

$$v'_n\{2\} = \frac{d_n\{2\}}{\sqrt{c_n\{2\}}}. \tag{21}$$

Because the POIs in this thesis are selected based on their transverse momentum, I will denote the differential flow with $v_n(p_{\mathrm{T}})$.

3.2 The algorithm

In the previous section we explored the definitions of integrated and differential flow as presented in Ref.[7]. Now I will introduce the algorithm used to calculate the correlations between different order harmonics. This algorithm is the second of two algorithms introduced in Ref.[1]. In order to explain it, we begin with the definition of the weighted single-event averaged multi-particle correlation:

$$\begin{aligned} \langle m \rangle_{n_1,n_2,\ldots,n_m} &\equiv \langle e^{i(n_1\phi_{k_1}+n_2\phi_{k_2}+\cdots+n_m\phi_{k_m})} \rangle \\ &\equiv \frac{\sum\limits_{k_1,k_2,\ldots,k_m=1}^{M}{}' w_{k_1} w_{k_2} \cdots w_{k_m} e^{i(n_1\phi_{k_1}+n_2\phi_{k_2}+\cdots+n_m\phi_{k_m})}}{\sum\limits_{k_1,k_2,\ldots,k_m=1}^{M}{}' w_{k_1} w_{k_2} \cdots w_{k_m}}, \end{aligned} \tag{22}$$

where $n_1, n_2, \ldots, n_m$ are the harmonics to be correlated, M is the multiplicity of the event, ϕ labels the azimuthal angles of the particles, and w labels the particle weights. In this thesis weights were not used, but they are needed for proper construction of the general framework. The prime behind the summation signs once again indicates no repeated indices. Since for this theory weights are used, I will also introduce the weighted Q-vector:

$$Q_{n,p} \equiv \sum_{k=1}^{M} w_k^p e^{in\phi_k}, \tag{23}$$

where n denotes the order of harmonic, and p the power of the weights. Now we can define the algorithm, starting with some shortcuts for ease of writing. We split Eq.22 into its numerator and denominator:

$$N\langle m\rangle_{n_1,n_2,\ldots,n_m} \equiv \sum_{k_1,k_2,\ldots,k_m=1}^{M}{}' w_{k_1}w_{k_2}\cdots w_{k_m}e^{i(n_1\phi_{k_1}+n_2\phi_{k_2}+\cdots+n_m\phi_{k_m})}, \tag{24}$$

$$D\langle m\rangle_{n_1,n_2,\ldots,n_m} \equiv \sum_{k_1,k_2,\ldots,k_m=1}^{M}{}' w_{k_1}w_{k_2}\cdots w_{k_m} = N\langle m\rangle_{0,0,\ldots,0}. \tag{25}$$

Because the denominator is easily obtained from the numerator by setting all harmonics to zero, it is omitted in further discussion on the algorithm. The innermost sum can be rewritten without the constraint of not being equal to any other index as the following:

$$\begin{aligned} N\langle m\rangle_{n_1,n_2,\ldots,n_m} = &\sum_{k_1,k_2,\ldots,k_{m-1}=1}^{M}{}' w_{k_1}w_{k_2}\cdots w_{k_{m-1}}e^{i(n_1\phi_{k_1}+n_2\phi_{k_2}+\cdots+n_m\phi_{k_{m-1}})} \\ &\times\Big(\sum_{k_m=1}^{M} w_{k_m}e^{in_m\phi_{k_m}} - \sum_{j=1}^{m-1} w_{k_j}e^{in_m\phi_{k_j}}\Big). \end{aligned} \tag{26}$$

This can be expanded into the following recursive formula:

$$\begin{aligned} N\langle m\rangle_{n_1,n_2,\ldots,n_m} = {} & Q_{n_m,1}N\langle m-1\rangle_{n_1,n_2,\ldots,n_m-1} - N\langle m\rangle_{n_1+n_m,n_2,\ldots,n_{m-1}} \\ & - N\langle m-1\rangle_{n_1,n_2+n_m,\ldots,n_{m-1}} - \ldots - N\langle m-1\rangle_{n_1,n_2,\ldots,n_{m-1}+n_m}, \end{aligned} \tag{27}$$

from this the algorithm can be derived. The authors of Ref.[1] have provided a code package that can be used with ROOT to implement this algorithm for calculations up to and including $m = 8$, the URL to download the package can be found in their paper. The algorithm is outlined in pseudo-code below, initially all $c_i = 1$:

$\mathrm{N}\langle 1\rangle'_{n_1}(\{c_1\})$: return Q_{n_1,c_1}
$\mathrm{N}\langle m\rangle'_{n_1,\ldots,n_m}(\{c_1,\ldots,c_m\})$:
  $C \leftarrow Q_{n_m,c_m}\times\mathrm{N}\langle m-1\rangle'_{n_1,\ldots,n_{m-1}}(\{c_1,\ldots,c_{m-1}\})$
  if $c_m \leq 1$ then
    for $i \leftarrow 1, m-1$ do
      $C \leftarrow C - c_i\times\mathrm{N}\langle m-1\rangle'_{n_1,\ldots,n_i+n_m,\ldots,n_{m-1}}(\{c_1,\ldots,c_i+1,\ldots,c_{m-1}\})$
    end for i
  end if
  return C .

(28)

More details on the algorithms and their derivation and implementation can be found in Ref.[1]. One other important concept from this paper are the so-called *standard candles (SC)*. It starts off with the following four-particle correlation:

$$\langle\langle\cos(m\phi_1 + n\phi_2 - m\phi_3 - n\phi_4)\rangle\rangle, \tag{29}$$

then the constraint $m \neq n$ is imposed. The isotropic part of the four-particle cumulant is given by:

$$\begin{aligned}\langle\langle\cos(m\phi_1 + n\phi_2 - m\phi_3 - n\phi_4)\rangle\rangle_c &= \langle\langle\cos(m\phi_1 + n\phi_2 - m\phi_3 - n\phi_4)\rangle\rangle \\ &\quad - \langle\langle\cos[m(\phi_1 - \phi_2)]\rangle\rangle\langle\langle\cos[n(\phi_1 - \phi_2)]\rangle\rangle \\ &= \langle v_m^2 v_n^2\rangle - \langle v_m^2\rangle\langle v_n^2\rangle \\ &= 0.\end{aligned} \tag{30}$$

The double brackets once again indicate averaging over all events. Due to the condition that $m \neq n$, a lot of terms which appear in the general cumulant expansion, such as $\langle\langle\cos[m(\phi_1 - \phi_2)]\rangle\rangle$, are non-isotropic, because of this they average to zero when averaged over all events. If the values of v_m and v_n are fixed over all events, the four particle cumulant as defined above is zero by definition. The same thing happens when these two harmonics are uncorrelated, since the expression $\langle v_m^2 v_n^2\rangle$ can then be factorized. Taking all of this into account, this four-particle cumulant is non-zero only if the event by event fluctuations of v_m and v_n are correlated. Therefore, measurement of this *standard candle* can be used to estimate the correlations between two different flow harmonics. By combining this concept with the algorithm above, we get a method for calculating the SC's without using direct calculations. The notation for these correlations is SC(m,n) with m and n representing the different harmonics, so SC(4,2) would be the correlation between v_2 and v_4.

4 Results

Now that we have covered how the data was recorded and how it was analysed, we can get into the results. I will begin by showing the results of the estimations of the integrated and differential flow. The integrated flow was calculated for the 2^{nd}, 3^{rd} and 4^{th} order harmonics, the differential flow was calculated only for the 2^{nd} order harmonic. The integrated flow is plotted in Fig.3, and the differential flow is plotted in Fig.4. We can see in Fig.3 that the 2^{nd} order harmonics is the largest, followed by the 3^{rd} and 4^{th} order. There is also an increase in the value of all three harmonics as the centrality increases. In Fig.4 we see an initial increase in the value of $v_2\{p_{\text{T}}\}$ with p_{T} up to a value of 3.75 Gev/c, then it starts to decrease. As a side note, the errors on these values are smaller than the marker size. Now we get into the results of the algorithm, shown in Fig.5. Here we can see that the flow harmonics have much smaller correlations according to the estimation made by the algorithm, in comparison to estimations made by the authors of Ref.[9]. They only estimated the correlations between the 2^{nd} and 4^{th}, and the 2^{nd} and 3^{rd} order harmonics, so there are no results that can be used to compare the estimation of SC(4,3) to.

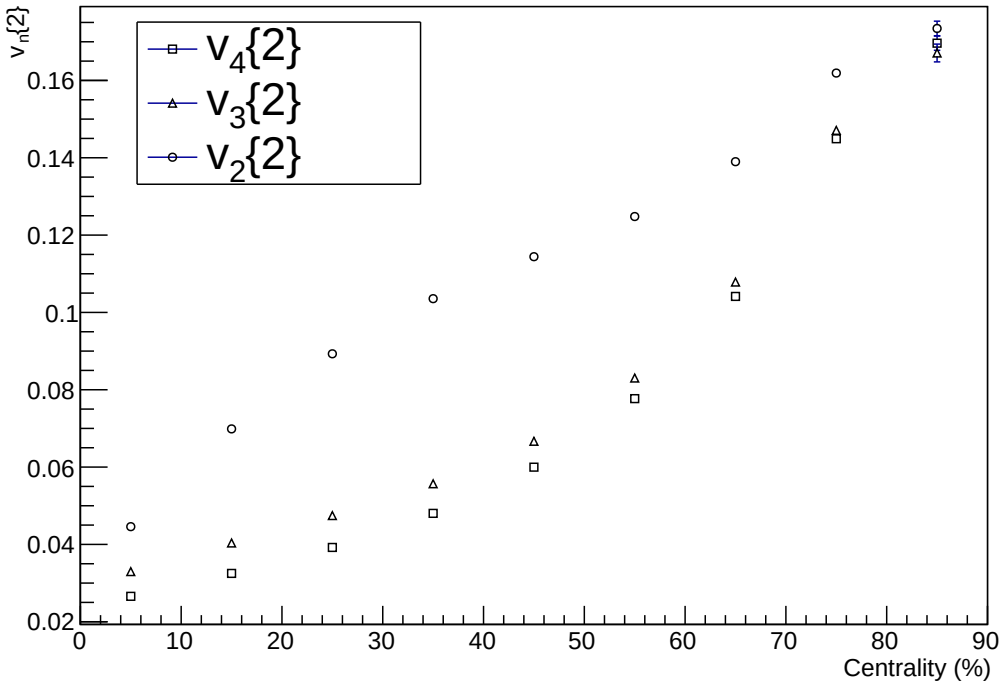

Figure 3: 2nd, 3rd and 4th order integrated flow harmonics, as a function of the centrality, with $0.2 < p_{\mathrm{T}} < 50\,\mathrm{GeV}/c$ and $|\eta| < 0.8$.

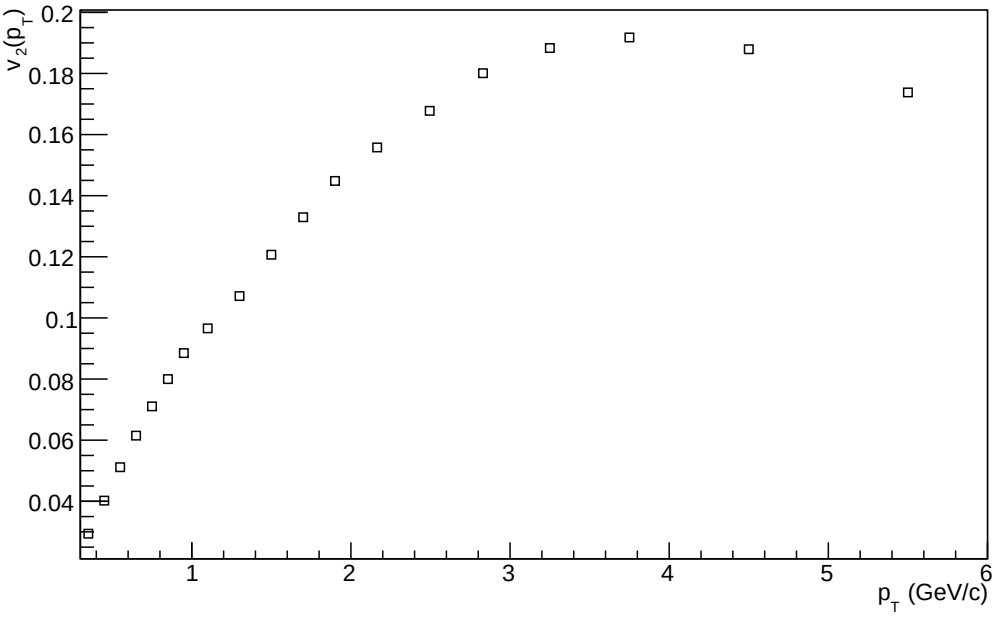

Figure 4: 2nd order harmonic differential flow in the 20-30% centrality range and $|\eta| < 0.8$.

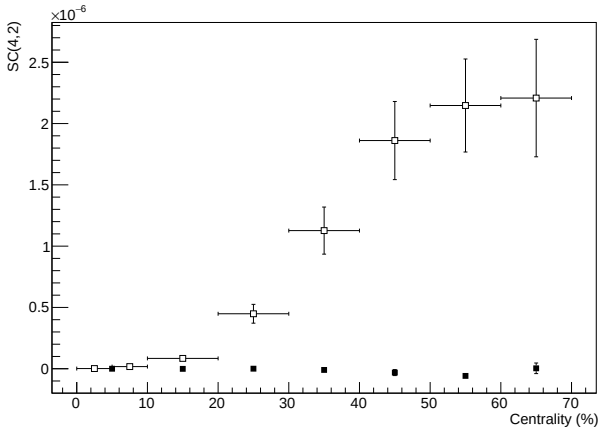

(a) SC(4,2)

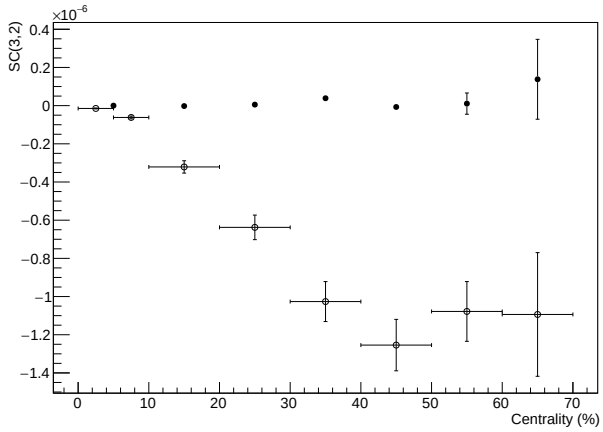

(b) SC(3,2)

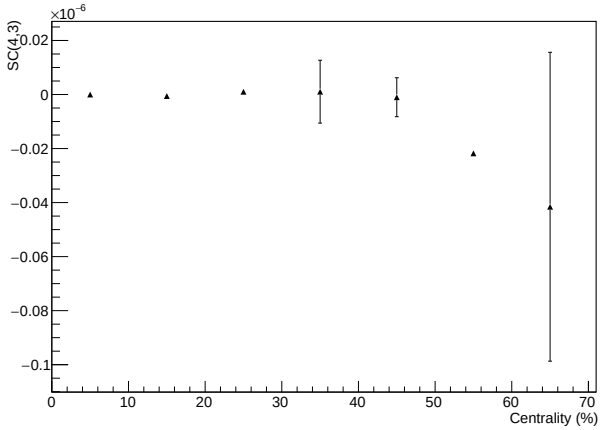

(c) SC(4,3)

Figure 5: The estimations for the correlations between the flow harmonics as function of the centrality, as estimated by the algorithm from Section 3.2. The solid markers are the values as estimated by the algorithm, the open markers, if present, are values for the same correlations as calculated by the authors of Ref.[9].

5 Conclusions, discussion, and outlook

Now that we have covered all the topics needed to answer the research question, we can get to answering it and discussing the possible reasons why the algorithm failed or succeeded. Some suggestions for possible future research into this topic are also made.

5.1 Conclusions

We start of by drawing conclusions on the results obtained and the answering the research question. The question that was asked at the beginning of this thesis was:

> Is this algorithm a good method for calculating correlations in flow harmonics?

The criteria for this algorithm had to fulfil before we could call it good, were the following:

- Is it compact?
- Is it fast?
- Is it accurate?

The most important of these three conditions is accuracy. It is of little use to have a fast and compact algorithm, if it does not produce accurate results. As we can see from the results, it is not accurate. The estimations it made for the SC's are nowhere near the values found in previous research. As such the conclusion here is that, no, the algorithm is not accurate. As for the other two criteria, the algorithm was reasonably compact. There were multiple files needed to implement it, but it did not require many lines of code to use it, compared with using direct calculations. As for its speed, there wasn't really anything for me to compare it to, but it ran the calculations on the entire set of 16 million events in a little under 6 hours. This allowed me to do multiple runs on the data to optimize my code, and to correct some possible errors that were made during implementation. So the answer to the main question is, no, this algorithm is not a good method for calculating correlations in flow harmonics. The reason for this is that it failed to produce accurate estimations of the correlations.
On the other hand, the estimation on the flow harmonics themselves did show trends that match the expectations, both for the integrated, and the differential flow. The expectations for the integrated flow were an increase with centrality due to the more elliptical nature of the impact area of two colliding particles when the centrality increases. These results for the flow harmonics show that the data that was recorded is good, and that the fault with the estimations of the algorithm most likely lies in its implementation.

5.2 Discussion and suggestions

The one thing that caused me the most problems was the actual implementation of the algorithm itself. This was mostly to do with my inexperience with coding, and partly with the comments provided to explain the code that I tried to implement. From this code itself it also wasn't entirely clear which quantity it calculated. Whether this was the entire SC itself or only $\langle v_m^2 v_n^2 \rangle$ wasn't clear. The results shown in this thesis were calculated in assumption

of the latter. Multiple attempts were made to find out what quantity it calculated but all of these did not produce accurate results. The results shown were chosen mostly because they seemed to be the most promising when testing the code on a toy Monte-Carlo model, the steps taken during this testing can be found in Appendix A. One other missed opportunity was the use of particle weights, that can be used to correct for non-uniform track reconstruction efficiency. They were not used in this thesis but they might have produced different results, which in turn could have been more similar to what was found in previous research. One other option would have been to consult the authors of the algorithm, however, time did not allow for this.

So some suggestions can be made to improve the results from this thesis, or for future research to be done. A more in depth look at the structure of the code provided could offer some clarity on the results it produces, which could lead to a different implementation and better estimations of the SC's. Using particle weights could also improve these estimations. When the algorithm does prove to be successful it could be used for calculations of correlations with more than 4 particles, it is there that the most profit could be gained from using this algorithm opposed to using direct calculations, which become quite cumbersome for many particles. This could lead to more accurate estimations of the correlations, that could give rise to a better understanding of how the anisotropies observed are linked to the initial conditions of high energy heavy ion collisions.

References

[1] A. Bilandzic, C. H. Christensen, K. Gulbrandsen, A. Hansen, and Y. Zhou, Phys. Rev. C **89**, 064904 (2014), URL https://link.aps.org/doi/10.1103/PhysRevC.89.064904.

[2] F. Gelis, J. Phys. Conf. Ser. **381**, 012021 (2012), 1110.1544.

[3] *Large hadron collider website*, URL https://home.cern/topics/large-hadron-collider.

[4] K. Aamodt, A. Abrahantes Quintana, R. Achenbach, S. Acounis, D. Adamova, C. Adler, M. Aggarwal, F. Agnese, G. Aglieri Rinella, Z. Ahammed, et al. (ALICE Collaboration), JINST **3**, S08002. 259 p (2008), also published by CERN Geneva in 2010, URL http://cds.cern.ch/record/1129812.

[5] R. Preghenella (ALICE), EPJ Web Conf. **49**, 02003 (2013), arxiv.org/abs/1302.0763.

[6] ROOT, *Root data analysis framework*, URL https://root.cern.ch.

[7] A. Bilandzic, R. Snellings, and S. Voloshin, Phys. Rev. C **83**, 044913 (2011), URL https://link.aps.org/doi/10.1103/PhysRevC.83.044913.

[8] U. Heinz and R. Snelling, Annu. Rev. Nucl. Part. Sci. **63**, 123 (2013), arxiv.org/abs/1301.2826.

[9] J. Adam, D. Adamová, M. M. Aggarwal, G. Aglieri Rinella, M. Agnello, N. Agrawal, Z. Ahammed, S. Ahmad, S. U. Ahn, S. Aiola, et al. (ALICE Collaboration), Phys. Rev. Lett. **117**, 182301 (2016), URL https://link.aps.org/doi/10.1103/PhysRevLett.117.182301.

A Toy Monte Carlo simulations

As mentioned before in Section 5, the results that are shown were chosen because of their promising results during testing with a Monte-Carlo (MC) model, that was used in order to develop the code and test different ways of implementing the algorithm. In this section we will discuss which steps were taken, and what the results were.
First some explanation on the implementation of the algorithm is in order. To use the algorithm in order to calculate the SC's first the harmonics had to be defined. This was done using vectors, for example, the vector (2,2,4,4) was used for calculating SC(4,2). These vectors are then used to define the Q-vectors that store the information on the particle tracks. At first the Q-vectors were defined by setting the maximum number of harmonics involved and the maximum power of weights. Using this method however caused the SC(4,3) to have values in the order of $\sim 10^{253}$ causing them to not be plotted at all, when the change was made to use the harmonic vectors to define the Q-vectors this issue was resolved. Having properly defined both the harmonic vectors and the filled Q-vectors, the correlations can be calculated. In this simulation the value of $v_2\{2\}$ was distributed continuously between 0.1 and 0.2. The values of $v_3\{2\}$ and $v_4\{2\}$ were then generated using a Gaussian distribution with an average of $-v_2\{2\}$ and $v_2\{2\}$ respectively, both with a standard deviation of 0.01. These values for the harmonics are then used to generate a set of angles which represent the tracks in the actual data.
After the first run over real data, it seemed that the SC's it calculated had the wrong sign. As a first step the order of harmonics in the vector were changed to see if this made a difference. So instead of defining the vector as (2,2,4,4) it was defined as (4,4,2,2) or some other permutation of these numbers. This seemed to make a difference at first, but when the MC was run using more events and tracks the estimations once again appeared to have the wrong sign. Up until this point it was assumed that the results that the algorithm produced were the SC's as defined in Eq.30. However, considering that the MC model did not produce the expected results and that the order in which the harmonics were defined did not seem to make a difference this was probably wrong. Finally, it was assumed that the value it calculated using the mixed 4-particle harmonic was not the SC, but instead $\langle v_m^2 v_n^2 \rangle$ as seen in the second to last line in Eq.30. So then 2-particle harmonics were also defined and used to calculate $\langle v_m^2 \rangle$. Using all this the SC's were finally calculated using the method from Eq.30. This then produced results that matched the expectations, as seen in Fig.6.

The final simulation was run using six different harmonic vectors, three defining the harmonics used in the 4-particle mixed harmonic correlator $\langle v_m^2 v_n^2 \rangle$, constructed as (m, n, m, n), and three defining the harmonics for the 2-particle correlators $\langle v_m^2 \rangle$. Using the 4-particle harmonic vectors three different Q-vectors were defined. Each one for storing the data for estimating a different SC. This was done to ensure that each of the Q-vectors was constructed as appropriate for the mixed harmonic it was defined from. The 2-particle correlations were also calculated from these Q-vectors, simulations were run to test whether or not using a different Q-vector made a difference, but this proved not to be the case. Using these six harmonics and three Q-vectors the SC's were estimated using Eq.30. These are also the settings used for generating the results from Fig.5.

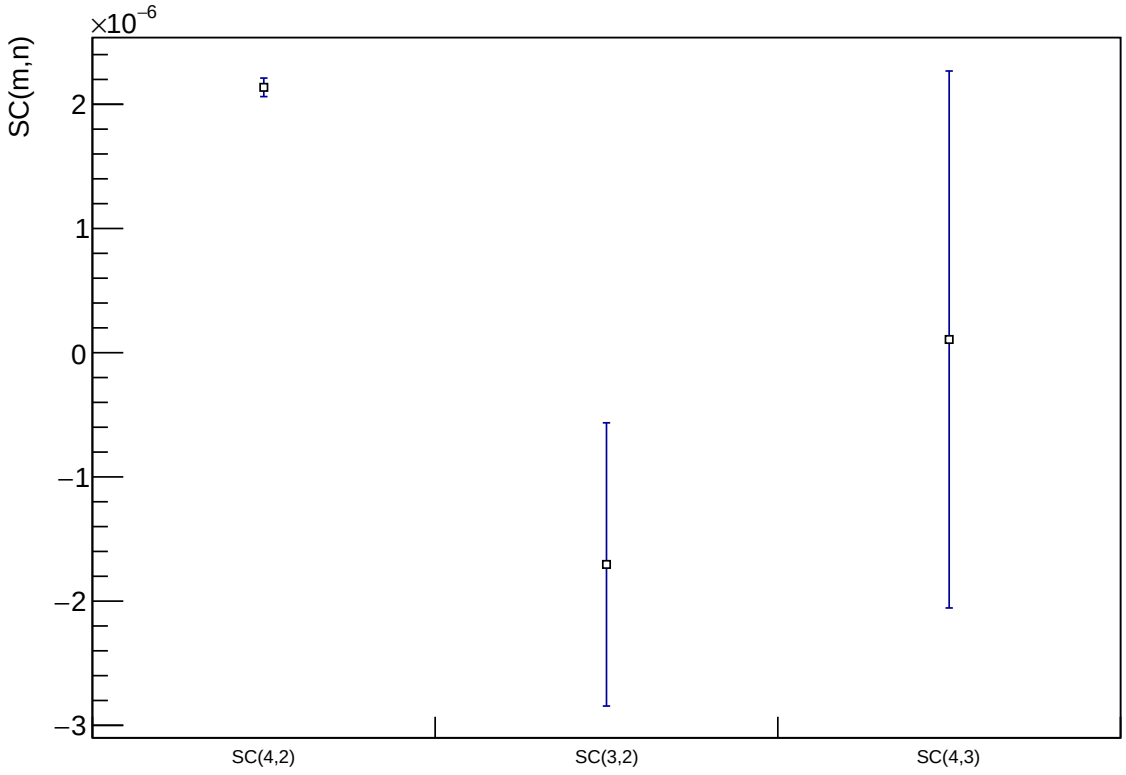

Figure 6: The results of the final MC simulation, with the SC's being calculated using multiple harmonics and Q-vectors.